

Effects of nonlinear propagation, cavitation, and boiling in lesion formation by high intensity focused ultrasound in a gel phantom

Vera A. Khokhlova^{a)}

*Department of Acoustics, Faculty of Physics, Moscow State University, Moscow, 119992, Russia
and Center for Industrial and Medical Ultrasound, Applied Physics Laboratory, University of Washington,
Seattle, Washington 98105*

Michael R. Bailey, Justin A. Reed, Bryan W. Cunitz,
Peter J. Kaczkowski, and Lawrence A. Crum

*Center for Industrial and Medical Ultrasound, Applied Physics Laboratory, University of Washington,
Seattle, Washington 98105*

(Received 8 January 2005; revised 5 December 2005; accepted 5 December 2005)

The importance of nonlinear acoustic wave propagation and ultrasound-induced cavitation in the acceleration of thermal lesion production by high intensity focused ultrasound was investigated experimentally and theoretically in a transparent protein-containing gel. A numerical model that accounted for nonlinear acoustic propagation was used to simulate experimental conditions. Various exposure regimes with equal total ultrasound energy but variable peak acoustic pressure were studied for single lesions and lesion stripes obtained by moving the transducer. Static overpressure was applied to suppress cavitation. Strong enhancement of lesion production was observed for high amplitude waves and was supported by modeling. Through overpressure experiments it was shown that both nonlinear propagation and cavitation mechanisms participate in accelerating lesion inception and growth. Using B-mode ultrasound, cavitation was observed at normal ambient pressure as weakly enhanced echogenicity in the focal region, but was not detected with overpressure. Formation of tadpole-shaped lesions, shifted toward the transducer, was always observed to be due to boiling. Boiling bubbles were visible in the gel and were evident as strongly echogenic regions in B-mode images. These experiments indicate that nonlinear propagation and cavitation accelerate heating, but no lesion displacement or distortion was observed in the absence of boiling. © 2006 Acoustical Society of America. [DOI: 10.1121/1.2161440]

PACS number(s): 43.80.Gx, 43.25.Yw, 43.25.Cb [CCC]

Pages: 1834–1848

I. INTRODUCTION

High intensity focused ultrasound (HIFU) is an emerging modern therapy in which ultrasound energy is locally absorbed in a millimeter-size focal region to induce tissue necrosis or cauterize bleeds without damaging intervening tissues. Current experimental and clinical therapies employ various noninvasive external (for treating brain, abdominal, bone, and ocular tumors, and for acoustic hemostasis), endoscopic and other intracavitary (for treating prostate and uterine tumors) methods as well as minimally invasive intravascular and intraoperative percutaneous techniques.¹ The main technical limitations to widespread clinical use of HIFU have been the long time required to treat tumors of typically several cubic centimeter volume,² the lack of developed real-time imaging methods for targeting and monitoring HIFU,³ and the large power demands that complicate portability for trauma applications such as battlefield hemostasis.⁴ Most clinical results to date have been obtained in China where over 10 000 cancer patients have been treated in the past 5 years.⁵ Many of these patients were treated with a HIFU

device that operates at very high acoustic intensity (more than 10 kW/cm²) combined with fast mechanical movement of the focus (several mm/s) over the tumor volume. The treatment site generally appears as a bright (echogenic) region in a B-mode ultrasound image, which is used for guiding the therapy.⁶

The use of B-mode ultrasound image-guidance while working with very high acoustic intensities and rapidly sweeping the focus was a successful innovation and appeared to be a practical solution to the first two problems of shortening treatment duration and monitoring the treated site in real time. Ultrasound image-guided HIFU devices have been developed for hemostasis and other applications.⁷ More sensitive ultrasound-based techniques are under development and MRI methods are also employed for targeting and monitoring the treatment.^{8–11} However, despite the existence of clinical devices, several important physical issues of nonlinear ultrasound-tissue interaction at this very high acoustic level remain poorly understood. These include the physical mechanisms responsible for the observed increase in volume and acceleration of tissue necrosis, and if this enhancement can be optimized by modifying the acoustic waveform to shorten treatment times or to reduce the energy requirements for portable trauma devices; the mechanism of lesion shape

^{a)}Author to whom correspondence should be addressed. Electronic mail: vera@acs366.phys.msu.ru

distortion from a symmetric “cigar” shape to a “tadpole” shape translated from the focus towards the transducer; accurate prediction of the final tissue damage; the origin of the echogenic region on a B-mode image and B-mode sensitivity in monitoring the treatment. This present work is intended to provide deeper insight towards answering these questions.

Two nonlinear effects are known to be involved in lesion production by HIFU: nonlinear acoustic wave propagation,^{4,12,13} and cavitation, i.e., ultrasound-induced oscillations of microbubbles grown from gaseous nuclei in tissue.^{14–16} The relative role of these two basic nonlinear phenomena is not yet well understood because models that fully represent heating response (and ultimately, biological response) to HIFU exposure in tissue do not exist. Both effects are expected to act simultaneously at high acoustic pressure and both are responsible for acceleration of lesion inception, overall growth, and distortion of the final lesion shape.^{17–19} The effect of acoustic nonlinearity results in generation of higher harmonics during propagation to the focus of the transducer, with shock formation under certain conditions for which acoustic energy is more effectively absorbed and converted to heat in the tissue.^{20,21} The presence of cavitation also leads to enhanced heating of tissue through the absorption of waves scattered or emitted by the bubbles (particularly as energy is often converted to higher, more readily absorbed frequencies), diffusion of heat from the hot compressed gas of the bubble interior, and viscous damping of bubble oscillations by the tissue or body fluids. The relative importance of these three cavitation mediated mechanisms is currently under investigation.^{16,22}

In addition to cavitation, bubbles in tissue may form from boiling. Boiling, that is, the growth of vapor bubbles occurs due to HIFU-induced temperature rise. In this sense, boiling is to be distinguished from cavitation which occurs due to HIFU-induced pressure oscillations. Cavitation bubbles are expected to be small (resonant size is of the order of microns for HIFU frequencies) and predominantly gaseous, as the result of rectified diffusion.^{15,23} They might slowly grow by coalescence or enhanced outgassing from the fluid presumed to be saturated with gas due to elevated temperature, but they can also fission as a result of violent collapses called inertial cavitation. On the other hand, vapor bubbles created by boiling are not directly caused by pressure oscillations and thus can grow rapidly to a large size (on the order of millimeters). This growth is particularly explosive if super heating occurs as a result of rapid temperature increase. Several large boiling bubbles may scatter and reflect ultrasound much more effectively than a cavitating microbubble cloud. Strong reflections result in shielding the focus from HIFU energy and increased prefocal heating. Boiling bubbles, more so than cavitation bubbles, may therefore contribute to distortion of the lesion from a cigar shape into a tadpole shape and growth of the lesion toward the transducer.²⁴ Scattering from bubbles also produces a region of increased echogenicity on a B-mode image but it has been difficult to distinguish between cavitation bubbles and boiling bubbles while monitoring HIFU.^{3,25,26}

The goal of this work was to investigate experimentally and numerically the relative importance of acoustic nonlin-

earity and bubble dynamics (cavitation and boiling) in enhancement of heat deposition by HIFU, B-mode ultrasound imaging of treatment, and lesion dynamics. A transparent protein-containing gel phantom that turns optically diffusive as proteins denature was used to visualize heated volumes.²⁷ Here we refer to these whitish diffusive regions as lesions by analogy to bioeffects observed in tissue. Although it is not possible to directly transfer the results of observations in gel to real tissues, because some properties of gel differ from tissue, the gel permits direct optical visualization of lesion growth in real time (not possible in tissue) correlated with simultaneous observations using B-mode ultrasound (possible in tissue). Furthermore, numerical modeling of HIFU in gel indicates that the changes due to nonlinear propagation are relatively greater than in tissue thus facilitating the observation of physical processes involved in lesion dynamics. The appearance of large bubbles, for example, due to boiling, can clearly be observed in the gel, even inside the diffusive lesion under backlighting conditions.

Experiments were conducted in two different physical arrangements. In the first set of experiments, in addition to single point lesions it was possible to produce lesion stripes, but only under standard atmospheric pressure. In the second set of experiments, elevated static pressure was used to suppress cavitation and boiling, but only single lesions were produced due to size constraints of the hyperbaric chamber. Different nonlinear regimes of heating were studied based on the same time-average acoustic power of the transducer but different pulse power (peak pressure). Metrics of lesion inception time, lesion growth rate, the appearance of bubbles, and morphological change of the lesion from symmetric cigar to distorted tadpole shape were used to characterize different regimes and stages of lesion dynamics.

II. EXPERIMENTAL METHODS

A. Tissue-mimicking phantom

An optically transparent polyacrylamide gel containing Bovine Serum albumin (BSA) was used in experiments as a tissue-mimicking phantom. The transparent gel turns translucent at high temperatures near 60 °C due to the presence of BSA proteins that become optically diffusive when thermally denatured. Table I lists the ingredients and proportions required to create a 200 ml gel with 7% concentration of BSA. This recipe was recently developed for use as a thermal in-

TABLE I. Chemical composition of 200 ml polyacrylamide gel with 7% BSA concentration.

	ml	Percent
Total volume	200.000	
Distilled water	143.220	0.7161
1 M TRIS	20.000	0.1000
40% Acrylamide	35.000	0.1750
10% APS	1.680	0.0084
TEMED	0.100	0.0005
	Grams	
BSA	14	7.000

dicating phantom for HIFU,²⁷ and it is included here for completeness. The gel phantoms were prepared by first mixing the BSA protein (Sigma-Aldrich) in distilled water degassed by pinhole degassing. The solution was gently stirred to mix the BSA powder, which likely reintroduced some gas. A solution of acrylamide then was added to the mixture, followed by a 1M TRIS buffer pH 8 (trizma hydrochloride and trizma base, Sigma-Aldrich), and the APS (ammonium persulfate, Sigma-Aldrich). The entire solution was placed in a vacuum chamber and held under vacuum of 700 mm Hg strength for over 1 hour for additional degassing. The final polymerization agent was degassed in a vacuum chamber and added to the remaining solution which was then transferred into cylindrical or cubical molds, and allowed to polymerize under vacuum. For comparison, some gels were made without degassing the ingredients. The gels have a useful lifetime of several weeks and these experiments were conducted the day of manufacture or the gels were vacuum-sealed in plastic bags, stored at 5 °C, and used the next day.

It has been shown that the acoustical and thermal properties of the gel are similar to those of tissue, although the acoustic attenuation in gel with 7% BSA is about one-third of the value in tissue.²⁷ Higher protein concentration would result in stronger absorption, but less transparency of the gel which becomes cloudy. Using a higher percentage of acrylamide makes the gel stiffer but does not appreciably increase attenuation; furthermore, the exothermic polymerization reaction becomes too hot to prevent denaturation of the BSA during gel preparation.

B. Experimental arrangement for lesion stripes

For the first set of experiments, performed under atmospheric pressure, the experimental arrangement presented in Fig. 1 allowed production of both static lesions and lesion stripes obtained by linearly translating the ultrasound trans-

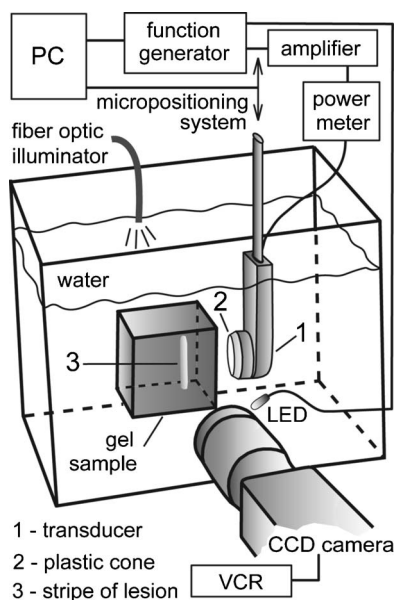


FIG. 1. Experimental arrangement for video imaging of HIFU-induced single lesions and lesion stripes in gel phantom. The transducer of 3.5 MHz frequency, 33 mm aperture, and 35 mm focal length was translated vertically at a constant velocity while HIFU was on.

ducer. A cubical gel sample of 5.5 cm on a side was mounted in a large water tank at room temperature (22 °C). The water in the tank was degassed for 2 hours prior to the measurements, which resulted in an air saturation level of less than 25% measured by a dissolved oxygen meter (YSI, Yellow Springs, Ohio). The sample was held in position by an acrylic box with open sides facing and opposite the transducer to prevent reflection from the acrylic. A CCD camera was used to film lesion formation with fiber optic lighting from above, and to record the image to VHS video tape. An LED placed in the field of view of the CCD indicated when the HIFU was on. Videotapes were later digitized by an ATI video capture board and software. Observation time of different stages of lesion development was determined by counting video frames (30 fps).

The transducer (SU-107 Sonic Concepts, Woodinville, WA) had a 3.5 MHz single element with 33 mm aperture and 35 mm radius of curvature. A truncated hollow acrylic cone larger than the acoustic beam width of the HIFU was used to aid in alignment and to hold a thin polyethylene film to suppress the development of streaming in the water path between the transducer and the sample. The transducer was affixed to a computer controlled 3-axis positioning system and a LABView (National Instruments, Austin, TX) program was written to control the experiment, including setting the timing and communicating the desired signal amplitude to the HP 33120 function generator via GPIB. The RF signal generated by the function generator was amplified by a linear 150 W RF amplifier (ENI A150). Forward RF power was monitored by a power meter (Sonic Concepts, Woodinville, WA) that measured voltage and current, and displayed true time-averaged electric power into the transducer. For comparison to the results of modeling the transducer was calibrated by a radiation force balance method to measure acoustic power output versus electrical power input at the levels of ultrasound used in the experiments. The efficiency was found to be 84% ± 4%. The ultrasound beam pattern was also measured in water using a calibrated needle hydrophone (SEA model GL-0150-1A with 150 μm active area, Soquel, CA) at low power to ensure a good match of the experimental pressure field geometry with the predictions of the theoretical model.

For static single lesions, preliminary experiments were performed in continuous wave (cw) regime with gradually increased transducer power to observe the changes in lesion inception and further growth. A baseline power value was empirically selected such that a lesion appeared in 4 seconds, which is a typical exposure for HIFU applications. For higher power levels, small steps in power increase were used to observe the appearance of bubbles and qualitative changes in lesion dynamics within the 4 second exposure. Further measurements were conducted with variation of pulse acoustic power combined either with the same exposure time (4 seconds) and different duty cycle, or with different exposure times with cw exposure, such that equal total acoustic energy was transmitted into the gel. When the duty cycle was less than 100%, the value of pulse acoustic power was obtained by dividing the cw power level of the transducer by the chosen duty factor to keep the same time-averaged value of

acoustic power. The pulse repetition frequency for the duty cycle regime was 1 kHz, and the duty cycle varied from 100% to 50%, with corresponding doubling of the pulse power level. The idea of exploiting nonlinearity to enhance heating with constant energy input (by varying duty cycle) has been presented earlier.^{12,28}

When producing stripes of lesions, the LABView program was used to control the speed with which the transducer was translated and to turn on the HIFU only when the transducer was not accelerating. Signal generation was initiated with some delay to permit the transducer to reach a steady speed. To maintain a regime of equal acoustic energy radiated into the gel, the stripes were produced with variation of duty cycle (100%–6.25% with 1 kHz repetition rate) combined either with the same transducer velocity (0.5 mm/s) and different pulse acoustic power (15–240 W), or by varying transducer velocity (0.5–6 mm/s) and preserving constant acoustic power. The power regimes were chosen based on the results of the experiments with single lesions so as to produce a visible small trace of lesion in cw regime at the lowest level of power (least nonlinear acoustic regime) at the slowest velocity of the transducer. Then the pulse power was increased incrementally in proportion to the decrease of the duty cycle or transducer velocity to maintain the same time-average acoustic power. Transducer velocity was chosen within the range of the ones typically used in clinical HIFU.^{5,6} Both degassed and nondegassed gel samples were compared to evaluate the utility of degassing in gel preparation.

C. Experimental arrangement for overpressure

The goal of the second set of experiments was to apply static overpressure to isolate the effect of nonlinear propagation from the effect of bubbles in enhancement of heat deposition. Overpressure (elevated hydrostatic pressure) dissolves existing bubbles, raises the boiling temperature, and restricts the activity of any HIFU induced microbubbles or boiling bubbles that may form in gel. The experimental arrangement is shown in Fig. 2. An aluminum pressure chamber was built using a 10 by 12.5 by 15 cm aluminum block with two cross-

ing bore holes of 5 cm and 6.2 cm diameter made on perpendicular sides of the chamber. The chamber can withstand an overpressure of more than 120 bars. Cylindrical gel samples were 6 cm in diameter by 6 cm long. The gel sample sat in the larger diameter horizontal bore hole with degassed water added to fill the remaining volume of the chamber. An oil-backed, piezoceramic, axially symmetric spherically shaped HIFU transducer of 2 MHz frequency, 40 mm aperture, and 44 mm radius of curvature was mounted on the right-hand side of the chamber closing one end of the other bore hole. Opposite the HIFU transducer, on the left-hand side, was a 2.5 cm thick transparent acrylic window. Two more acrylic windows of the same thickness capped both ends of the larger bore hole on the front and back sides of the chamber. A fiber optic light was used to illuminate the sample either from the side through the left-hand acrylic window or from the back through a diffusive sheet of white paper placed close to the window. Lesion formation was filmed by a CCD camera through the front window of the chamber. In this set of experiments, the A150 amplifier was replaced by an AP400B model because the transducer efficiency (39% ± 4%) and frequency were lower than that of the SU-107 transducer. The transducer was calibrated as before, using combined radiation force balance, field mapping, and modeling tools; electric power was monitored during experiments using the power meter.

The hydraulic hand pump (Ralston Instruments, Chagrin Falls, Ohio) was used to apply pressure to the water-filled interior of the closed pressure chamber with the gel sample inside. A fluid conduit connected the water to the oil that filled small high pressure transducer housing and insulated the backside of the transducer element. A free piston inside the conduit prevented mixing of the two fluids while permitting equalization of pressure between oil and water, and thus across the brittle transducer element. An electrical network matched the transducer to 50 Ohms, but no acoustic matching layer was developed for the transducer face. Net electrical power to the transducer was measured and was the same with and without overpressure.

Modifications were made to the acrylic caps of the chamber (not shown in Fig. 2) to make additional measurements with an ATL HDI-1000 ultrasound system (Philips, Bothell, WA) which was used to record B-mode images to SVHS video tape. The C4-2 broadband diagnostic imaging probe with 3 MHz central frequency and 2–4 MHz bandwidth was affixed to the chamber and coupled by commercial ultrasound coupling gel at the rear acrylic window to monitor the treatment and to correlate B-mode images with visual observations. The alignment of the imaging focus and the HIFU focus was performed by imaging the opposite chamber window. In order not to saturate the B-mode image with HIFU, the HIFU was synchronized to the imager frame rate (32 Hz), run at 50%–72% duty cycle (except under cw), and phased so that the interference was relegated to the edges of the image.

To assess the presence of cavitation for the experiments at ambient static pressure additional cavitation measurements were performed outside the pressure chamber for degassed gel samples. A passive cavitation detection (PCD) system

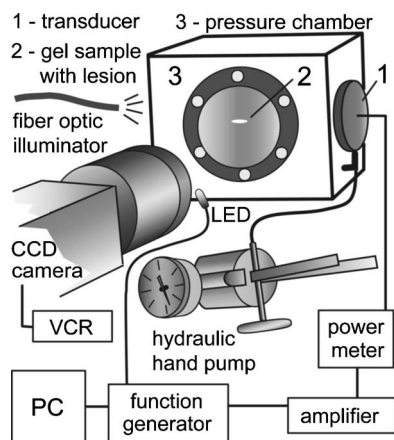


FIG. 2. Experimental arrangement for video imaging of HIFU-induced single lesions in gel under elevated static pressure. The transducer was of 2 MHz frequency, 40 mm aperture, and 44 mm focal length.

consisted of a 20 MHz focused transducer (Staveley Sensors Inc., East Hartford, CT) aligned confocally and with its axis perpendicular to HIFU, a 15 MHz high-pass filter (Allen Avionics Inc., Mineola, NY), a preamplifier (Panametrics-NDT Inc., Waltham, MA), and a Lecroy LT344 oscilloscope (Chestnut Ridge, NY). A 200 cycle burst was sent from the HIFU source at increasing power levels and the resulting PCD traces were recorded. The onset of cavitation was correlated with a dramatic change in PCD signal level. Using this system, it was found that the cavitation threshold of the degassed, 7% BSA-polyacrylamide gel varied over the range from 2 to 16 W acoustic power of the HIFU source, depending on how carefully the ingredients of the gel were degassed. This power range corresponds to acoustic peak negative pressure of 2–6 MPa in the gel at the focus, obtained from the results of nonlinear modeling.

All the experiments in overpressure chamber (at ambient pressure) were always performed well above the cavitation threshold and consequently cavitation was presumed to occur for all atmospheric pressure exposures. The peak acoustic power varied from 25 to 75 W and from 100% to 50% duty cycles, with a 30 s exposure that was empirically determined to provide observations of a qualitatively varied range of lesion development regimes, with and without overpressure. For overpressure experiments, samples were pressurized and maintained at pressure for 5 minutes prior to HIFU exposure to allow ample time for ambient bubbles to dissolve. In most of these experiments the level of overpressure was chosen to exceed the peak negative pressure at the HIFU focus to completely suppress cavitation.

III. THEORY AND NUMERICAL MODEL

The experiments on single static lesion formation were simulated numerically with an assumption of either linear or nonlinear ultrasound propagation.

A. Linear and nonlinear acoustic field

The HIFU field was modeled using the KZK-type nonlinear parabolic equation, generalized for the frequency dependent absorption properties of the following propagation medium:

$$\frac{\partial}{\partial \tau} \left(\frac{\partial p}{\partial z} - \frac{\beta}{\rho_0 c_0^3} p \frac{\partial p}{\partial \tau} - L_{\text{abs}}(p) \right) = \frac{c_0}{2} \Delta_{\perp} p. \quad (1)$$

Here p is the acoustic pressure, z is the propagation coordinate along the axis of the beam, $\tau = t - z/c_0$ is the retarded time, c_0 is the sound speed, ρ_0 is the ambient density of medium, β is the coefficient of nonlinearity, $\Delta_{\perp} = \partial^2 / \partial r^2 + r^{-1} \partial / \partial r$ is the Laplacian with respect to the transverse coordinate r , L_{abs} is the linear operator that accounts for absorption and dispersion properties of the medium.

The propagation path for ultrasound was through a two-layer medium, first in water and then in the gel sample. For simulations in water, the thermoviscous absorption was included as

$$L_{\text{abs}} = \frac{b}{2c_0^3 \rho_0} \frac{\partial^2 p}{\partial \tau^2}, \quad (2)$$

where b is the dissipative parameter of water. For simulations in gel, the operator L_{abs} accounted for the power law of ultrasound absorption measured in the gel²⁷

$$\alpha(f) = \alpha_0 (f/f_0)^\eta \quad (3)$$

and variation of the sound speed with frequency calculated using the local dispersion relations²⁹ as

$$\frac{c(f) - c_0}{c_0} = \frac{c_0 \alpha_0}{\pi^2 (\eta - 1) f_0} \begin{cases} [(f/f_0)^{\eta-1} - 1], & \eta \neq 1, \\ \ln(f/f_0), & \eta = 1. \end{cases} \quad (4)$$

Here α_0 is the absorption coefficient and $c_0 = c(f_0)$ is chosen as the ambient sound speed at the fundamental frequency f_0 . Equation (1) was solved numerically in the frequency domain using a previously developed finite difference algorithm.^{21,30} The acoustic pressure waveform was represented as a Fourier series expansion; a set of nonlinear coupled differential equations for the amplitudes of harmonics was derived and integrated numerically using the method of fractional steps with an operator-splitting procedure.

Simulations were performed with and without acoustic nonlinearity in order to predict the importance of nonlinear propagation effects for particular experimental conditions. Spatial distributions of the amplitudes and the intensities I_n of the harmonics nf_0 , and the total intensity of the wave $I(z, r) = \sum_{n=1}^{\infty} I_n(z, r)$ were calculated. Acoustic waveforms were reconstructed at various distances from the transducer. Heat deposition patterns due to the absorption of ultrasound

$$q_v(z, r) = 2 \sum_{n=1}^{\infty} \alpha(nf_0) I_n(z, r) \quad (5)$$

were obtained for further simulations of the temperature rise in the gel.

The values of the physical constants used for the modeling were $\rho_0 = 1000 \text{ kg/m}^3$, $c_0 = 1486 \text{ m/s}$, $\beta = 3.5$, $b = 4.33 \times 10^{-3} \text{ kg s}^{-1} \text{ m}^{-1}$ for water; and $\rho_0 = 1044 \text{ kg/m}^3$, $c_0 = 1544 \text{ m/s}$, $\beta = 4.0$, $\alpha_0 = 1.6 \text{ m}^{-1}$ at 1 MHz, $\eta = 1$, for the gel.²⁷ No changes in the acoustic parameters of gel due to HIFU heating were considered in the simulations. The linear case was modeled by choosing $\beta = 0$.

B. Temperature field

Temperature rise in the gel phantom was modeled using a heat transfer equation

$$\frac{\partial T}{\partial t} = k \Delta T + \frac{q_v}{c_v}. \quad (6)$$

Here T is the temperature in the gel, c_v is the heat capacity per unit volume, k is the temperature conductivity, q_v is the distribution of thermal sources calculated from Eq. (5). Equation (6) was integrated numerically using a finite difference scheme.²¹ Thermal properties of the gel in simulations were $c_v = 5.3 \times 10^6 \text{ J m}^{-3} \text{ }^\circ\text{C}^{-1}$ and $k = 1.3 \times 10^{-7} \text{ m}^2 / \text{s}$.²⁷

A thermal dose required to produce a lesion in tissue has been defined³¹ but an analogous thermal dose for the BSA

gel is not well established. Preliminary experiments showed that gels turned optically diffusive in about 2 s at 58 °C and in less than 0.1 s at 65 °C.²⁷ These values are similar to those observed in tissue. Since the experiments and modeling were performed for rapid heating of gel with lesion inception time of the order of seconds, it was appropriate to choose a temperature rather than a time integrated thermal dose as a threshold of lesion inception. For calculations therefore we chose to model lesion formation by selecting a threshold temperature of 65 °C, at which the gel is considered to be instantly denatured. The lesion boundary defined in this way will be only slightly smaller than that which would be obtained by time integration.

IV. RESULTS AND DISCUSSION

A. Single lesions

The acoustic power threshold for formation of visible bubbles was found experimentally for a 4 second exposure by producing a sequence of lesions in degassed gel with gradually increasing HIFU power from 10 W to 20 W in the continuous wave (cw) regime. The lesions grew symmetrically until the end of the exposure for acoustic powers less than 16.5 W, at which formation of a big millimeter size bubble was observed (the threshold was sharp and repeatable). Figure 3 shows lesions observed in the gel at 2.5 s and 4 s for three acoustic powers close to this threshold of 16.5 W. It is seen that a very small increase in power yielded a sudden appearance of visible bubbles and corresponding significant change in lesion shape and size. The bubbles are far easier to perceive in a movie than in still images taken from the movie, but here we must present still images which were selected to best depict observations. Cigar-shaped symmetric lesions formed below a 16.5 W power threshold [Fig. 3(a)] and tadpole-shaped lesions with visible bubbles formed above the power threshold [Figs. 3(b) and 3(c)]. A large bubble was observed at the very end of the exposure at the edge of the lesion that faced the transducer for 16.5 W power [Fig. 3(b)]. Several bubbles developed in the lesion starting

from 2.5 seconds for 17 W power [Fig. 3(c)]. Bubbles appeared first in the center of the lesion along the transducer axis and quickly grew towards the transducer, causing the distortion of lesion size, position, and symmetry. Significant change in lesion inception time was also observed within this small change of acoustic power, 1.8 s for 16 W, 1.5 s for 16.5 W, and 1.1 s for 17 W acoustic power.

Rapid changes in lesion dynamics with a small increase of the source power suggested that nonlinear effects were involved at this level of HIFU. Further experiments were performed at “high” and “low” acoustic peak pressures with the same exposure duration of 4 s, the same time-average acoustic power of 16 W, but varying the pulse power and duty cycle appropriately, either in the cw regime or with 50% duty cycle at 1 kHz repetition rate. Substantial increase of the final lesion size, almost immediate (at 0.3 s) appearance of bubble activity, and translation of the lesion toward the transducer were produced by the high-amplitude waves compared to the smooth symmetric growth of the lesion produced by low-amplitude waves. Nondegassed gel samples were also treated under the same HIFU protocol without observable difference in lesion inception time and bubble appearance as compared to the degassed samples. We expected that if cavitation played a strong role, the lesion formation would proceed differently between degassed and gas saturated gels because of rectified diffusion. However, the dynamics of lesion growth was not strongly affected by the gas content dissolved in gel, unless the HIFU hit small, but visible bubbles remaining in nondegassed samples (these voids were absent in degassed gels), which resulted in some irregular distortion of the lesion. We have proposed⁴ and will elaborate here that sudden formation of visible bubbles in the lesion was due to boiling and that the fast change in lesion dynamics with a small increase of the HIFU power level was due to the formation of shocks and corresponding enhanced heating.

Similar “bubbly” structure of tadpole-shaped lesions has previously been observed visually in real tissues as cavities in the middle of the focal area and attributed to bubbles, either due to ultrasound-induced cavitation or to boiling.³² Figure 4 shows our observations of bubbly lesions in excised bovine liver. So-called “popcorn” claps, similar to boiling noise and presumed to be due to sudden phase change of superheated fluid, have been observed during tissue treatment above some intensity level of HIFU.³³ However, the relative importance of these two bubble mechanisms under different HIFU conditions is not well understood.

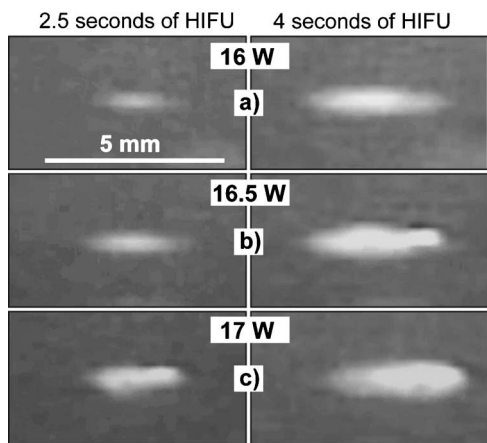


FIG. 3. Single lesions formed in degassed gel with 16 W (a), 16.5 W (b), and 17 W (c) acoustic power of the HIFU source after 2.5 s (left-hand set) and 4 s (right-hand set) exposure. The HIFU transducer was on the right-hand side. Slight increases in acoustic power cause accelerated lesion growth, then boiling, and then lesion distortion and migration toward the transducer.

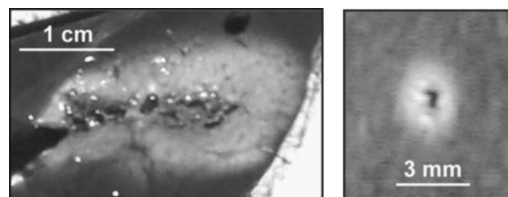


FIG. 4. Images of HIFU-induced overheated lesions in excised degassed bovine liver. Both an axial tadpole section (left-hand side) and a transverse section (right-hand side) of the lesions show vaporized cavities along the HIFU axis.

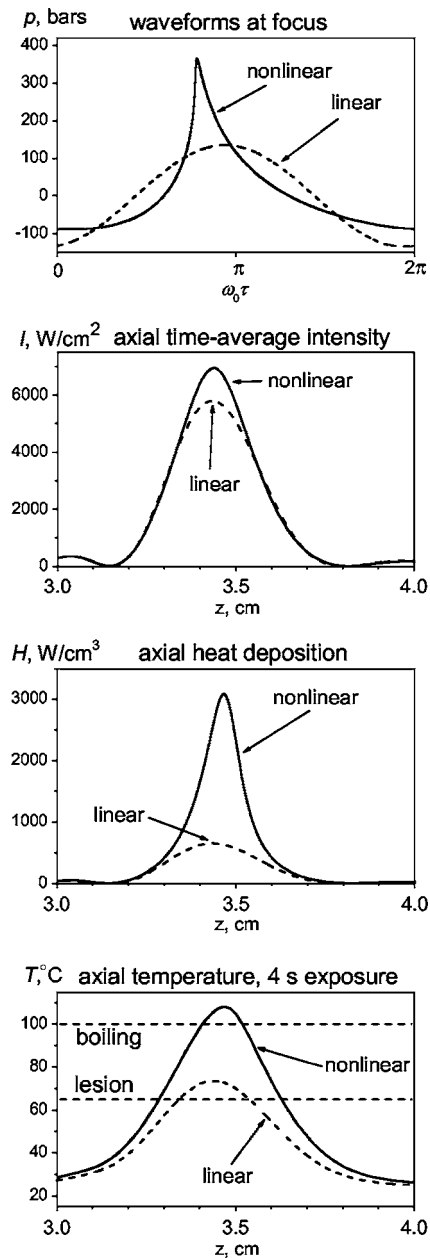


FIG. 5. Numerical results of modeling HIFU in gel with (solid lines) and without (dash lines) accounting for the effects of nonlinear propagation, axial waveforms at the focus; axial time-average intensity, heat deposition, and temperature rise after 4 s exposure. Acoustic power of the HIFU source in simulations was 16.5 W which corresponded to spatial peak intensity in gel of 5800 W/cm² calculated linearly. Accounting for nonlinear propagation predicts a shocked waveform, higher intensity and heat deposition, as well as boiling temperatures at focus as compared with the linear modeling.

To support the hypothesis of the effects of acoustic nonlinearity on enhanced heating and possible boiling of the gel, numerical simulations of gel heating were performed with and without nonlinear propagation effects for the conditions used in the experiments. Shown in Fig. 5 are the results of modeling of the acoustic and temperature field in the gel for an acoustic power of 16.5 W, the case in which a large bubble burst into the image at the end of the exposure [Fig. 3(b)]. The results of simulations show that at this power level of HIFU acoustic nonlinearity results in formation of a shock front in the acoustic waveform, weak enhancement of the

mean intensity, and a more than fourfold increase in heating at the focus of the HIFU source. Even though linear modeling yields axial temperatures in excess of 65 °C for 4 seconds of exposure, it fails to predict boiling (temperature rise to 100 °C or more) and overestimates the lesion inception time compared to that observed in the experiments. However, nonlinear modeling produces predictions of the onset of boiling and lesion inception time that closely agree with experimental results (within about 10%). Note, that whereas the peak heat deposition on the focal axis is increased fourfold by nonlinearity, the resulting peak temperature is increased by less than 50%. The nonlinearly enhanced peak of heating is spatially much narrower than the width of the linear HIFU acoustic beam; therefore much faster temperature rise is expected at the beginning of the exposure, but rapid diffusion of the steep temperature gradient smoothes the narrow nonlinear peak more quickly than in the linear case. HIFU intensities required for rapid lesion distortion and boiling observed in gels correlated well with numerical results for the onset of shock formation close to the focus, which gives additional support to the importance of the nonlinear propagation effect in enhanced heating.

The experiments with single lesions showed that for nonlinear regimes with equal time-average acoustic power, those with higher peak pressure resulted in faster heating, lesion inception, and appearance of large bubbles. Based on the results of this section which provide an excellent correlation between experimental observations and numerical simulations of nonlinear acoustics without cavitation effects, we attributed this sudden appearance of large bubbles to boiling, and distortion of lesion shape to reflections from these vapor bubbles.

B. Lesion stripes

Nonlinearly enhanced heating might be used to accelerate treatment of a tissue volume, such as a tumor which is typically much larger than a single focal lesion. One approach to treating a volume is formation of discrete single lesions with sufficient time between lesions for cooling; this controlled approach avoids boiling and distortion of lesion shape to produce predictable, symmetric lesions.²⁴ Moderate HIFU intensities of 1000–2000 W/cm² are typically applied. A second approach involves constant mechanical movement of the transducer with a velocity between 0.5 and 4 mm/s, a typical range for HIFU clinical studies.⁵ Much higher intensities are typically used to form lesion stripes in this approach and therefore nonlinear effects are expected to be more pronounced and thus benefit acceleration of the treatment. In addition to faster heating, formation of bubbles in the HIFU focal zone results in strong echogenicity that can serve to monitor the treatment. To examine the role of nonlinearly enhanced heating, lesion stripes were produced in gel by moving the ultrasound transducer. Two different regimes were employed. Variation of duty cycle was combined either with the same transducer velocity and different peak pressure (pulse power or intensity) or with different transducer velocity and the same pulse intensity. Both de-

gassed and degassed gel samples were treated to investigate the effect of gas concentration in the gel on lesion development.

In the first set of experiments, a series of seven lesion stripes separated spatially by 5 mm intervals were produced in one gel sample. The transducer was translated upwards at a velocity of 0.5 mm/s. Equal time-average acoustic power of 15 W was retained and duty cycle (dc) gradually increased with corresponding reduction of the peak power from 6.25% dc with 240 W pulse power, to 8.35%, 12.5%, 25%, 50%, 67%, and 100% with 15 W power. For the transducer velocity of 0.5 mm/s, the lowest power level for the cw regime was empirically chosen such that it was just sufficient to induce a symmetric lesion of minimal visible size and without the formation of boiling bubbles. Experiments with static exposures showed that a lesion became visible in 2 seconds and had a characteristic thickness of about 1 mm in 4 seconds at 15 W acoustic power without boiling, similar to the lesions shown in Fig. 3(a). A small increase in power from 15 to 17 W yielded boiling in 2.5 seconds, and doubling of the pulse power with the same average HIFU power of 16.5 W resulted in essentially immediate boiling in single lesion experiments. It was expected, therefore, that all the exposures producing stripes, except the lowest power and the cw regime, would produce observable nonlinear enhancement of heating and boiling. A fundamental difference between static and scanned exposures at a high pulse power level is that, while boiling begins in a very short time in both cases, it cannot persist and distort the lesion for scanned exposures because the focus of the transducer constantly moves away from the boiling site.

A photograph of a gel sample with seven lesion stripes is

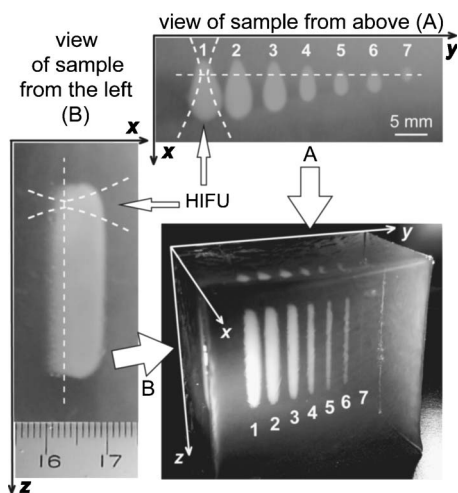


FIG. 6. Lesion stripes formed in degassed gel sample by moving the HIFU transducer upwards with constant velocity (0.5 mm/s), constant time-average acoustic power of the transducer (15 W), and different duty cycle (and peak power) from 6.25% (240 W peak power, 1) to 8.35% (2), 12.5% (3), 25% (4), 50% (5), 67% (6), and 100% (15 W peak power, 7). Ultrasound was applied from the front of the sample as indicated by HIFU arrows. The location of HIFU focal peak is shown by the straight dashed lines, and the general shape of the HIFU beam is shown by the curved dashed lines on the views of the sample from above (A) and from the left (B). Although the average power was held constant for each stripe, the stripes have very different sizes. The highest amplitude, shortest duty cycle pulses created the largest lesion stripe (1).

shown in Fig. 6. HIFU was applied from the front side of the sample. The photo on the left-hand side shows a side view of the largest lesion stripe (numbered 1) that corresponds to the highest pulse power level and lowest duty cycle. The geometry of the cross section of the lesions in the plane perpendicular to the direction of transducer movement is viewed from above of the sample. It is seen that much larger lesions both in length and width were produced for higher peak pressure (pulse power) levels for the same HIFU energy delivered to the sample. The biggest lesion (Fig. 6, number 1) was of 5 mm width and 10 mm length, whereas the smallest lesion (Fig. 6, number 7, only visible from the top) was of 1 mm width and 1.5 mm length. The waveform shape for given ultrasound energy thus dramatically changes resulting lesion size. Lesions produced by mechanically sweeping the transducer over the gel were larger for shorter, stronger pulses, indicating that higher amplitudes and shorter duty cycles cause enhanced heating.

The geometry of the lesion cross section transformed from the smallest (and symmetrical) lesion located at the focus of the transducer for the lowest peak pressures (7) into the drop-shaped lesions with centroids displaced from the focus toward the transducer. A dashed line on the top photograph corresponds to the peak focal intensity of HIFU and crosses the middle of the smallest lesion [Fig. 6 (lesion 7)]. It is seen that the lesion stripes 1–6, in which we expected boiling, are formed mainly proximally to the focus with a small increase of the lesion size distal to the focus [Fig. 6 (1–3)]. These results are consistent with the observations of lesions in tissue induced at high intensity levels^{18,19,33} and support the hypothesis that boiling and corresponding formation of large bubbles effectively reflect HIFU, and is the mechanism for the change in lesion shape from a “cigar” to a “drop” or “tadpole.” The stripe produced at the lowest peak pressure (7) was visually observed during the treatment as a moving hazy focal spot which immediately faded in opacity, though it could still be visualized many hours after the exposure.

To investigate the influence of gas content in gel (due to differences in preparation) and different regimes of lesion production, additional experiments were performed using 120 W pulse acoustic power applied to the degassed and nondegassed gels and varying the velocity of the transducer from 0.5 mm/s [Fig. 6 (3)] to 1, 2, and 4 mm/s. As before, the same acoustic energy radiated into the samples was maintained by increasing the duty cycle from 12.5% to 25%, 50%, and 100%, respectively. Under all these exposure conditions, boiling was expected to occur essentially immediately (within a small fraction of a second) given the prior empirical observations. Shown in Fig. 7 are the lesions obtained with 0.5 mm/s (the slowest) and 4 mm/s (the highest) scan velocity in degassed and nondegassed samples. The slower transducer movement resulted in formation of more uniform lesions [Figs. 7(a) and 7(b)]. More visible bubbles formed and remained in nondegassed gels [Figs. 7(b) and 7(d)]. The same differences were observed with the other transducer velocities of 1 and 2 mm/s, but they were more pronounced for the lesions obtained with the slowest and the fastest exposure (Fig. 7). The size of the lesions (size of the

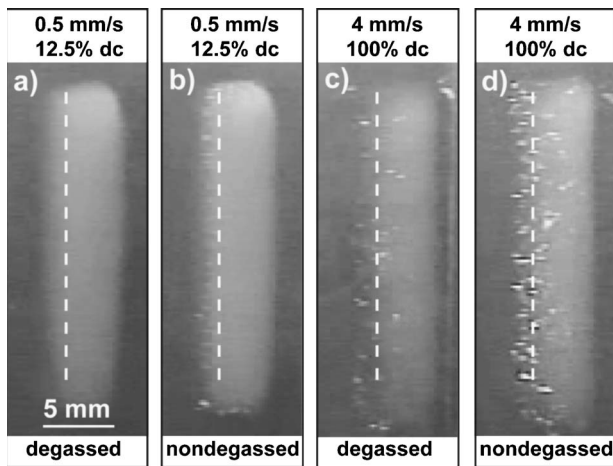


FIG. 7. Comparison of lesion stripes formed in degassed and nondegassed gel samples by moving the HIFU transducer upwards with different scan velocities of 0.5 and 4 mm/s. Insonation was from the right. Peak acoustic power was 120 W, the increase of the transducer velocity was compensated by increased duty cycle from 12.5% to 100% to maintain equal acoustic energy radiated into the sample to create one stripe. Dashed lines indicate the location of the HIFU focal peak. There are more visible bubbles sustained in the nondegassed gels and for faster scan velocity.

diffusive fogged zone) were very similar, however, the distal edge of the lesion was not uniformly treated for nondegassed samples and for higher transducer velocity. The bubbles visible at the distal end of the lesion were located close to the focus, and the proximal end had uniform structure. This suggests the following scenario for lesion development at the high intensity level: boiling starts almost immediately at the focus of the transducer and bubbles reflect ultrasound so that the region of maximum heating shifts toward the transducer. The gel continued to boil at the maximum of the heated region (on axis) but as the lesion grew thicker, boiling bubbles were no longer visible inside the lesion under the side-lighting conditions used in this experiment. In later experiments, a diffuse backlight that made boiling bubbles inside the lesion visible was used with the overpressure apparatus.

C. Overpressure

The results of simulations that accounted for acoustic nonlinearity showed locally enhanced heating leading to temperature rise sufficient for boiling, which correlated well with the experimental observations of single lesions in gel. Conversely, temperature rise obtained with the linear propagation model did not reach boiling at 100 °C. However, both linear and nonlinear simulations were performed with an absorption coefficient measured in gel at a low intensity level²⁷ and effective absorption at the focus at HIFU intensity might be higher due to the presence of cavitation (HIFU induced microbubbles too small to see), which would result in additional heating in the focal region compounding the effect of nonlinear propagation.

To isolate the effect of acoustic nonlinearity in gel heating from these two bubble-mediated mechanisms, a second set of experiments was conducted with a 2 MHz transducer in a hyperbaric chamber so that greatly elevated static pressure could be applied during HIFU exposure to suppress pos-

sible cavitation and increase boiling temperature. Lowering the frequency from 3.5 to 2 MHz was done to increase the role of cavitation by lowering the cavitation threshold at ambient static pressure and to induce slightly larger single lesions, given the larger focal beamwidth obtainable. Acoustic power was chosen so that all the experiments were performed in the presence of cavitation, which was confirmed by preliminary calibration measurements of cavitation threshold in the gel using a passive cavitation detector (PCD). In addition, as the linear absorption coefficient in the gel is nearly proportional to frequency, the difference in heating induced by shock waves versus linear monochromatic waves is stronger for lower fundamental frequencies.²¹ Further facilitating observations, the heating process at lower frequency in the linear regime (i.e., in the absence of the effects of nonlinear propagation or cavitation) should be slower, providing more time for the measurements. The changes in lesion development due to nonlinear effects were therefore expected to be more pronounced and more easily observed.

The goal of the initial experiments performed in the overpressure chamber under atmospheric pressure was to visualize characteristic stages of lesion development. Figure 8 represents a sequence of selected video frames for two gel

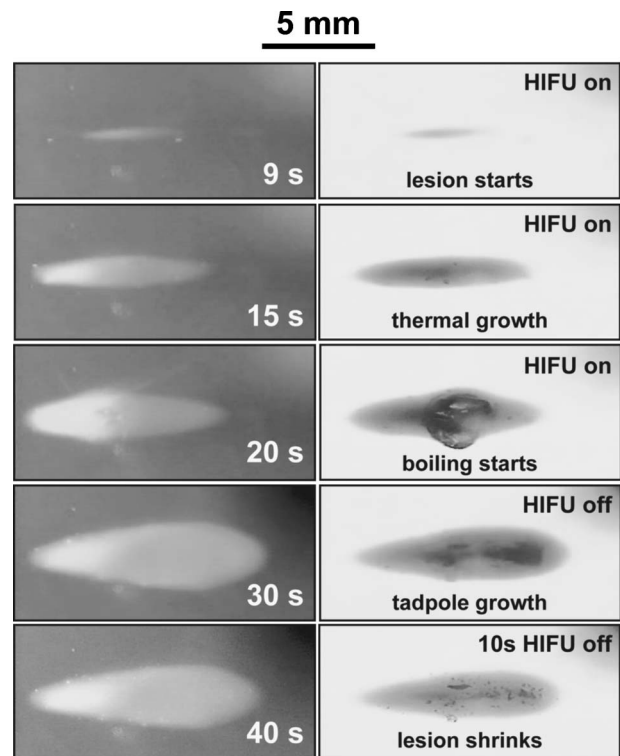


FIG. 8. Sequence of selected video frames illustrating different stages of lesion development in nondegassed gel: lesion inception (9 s after HIFU was on), thermal symmetric growth (15 s), asymmetric tadpole change of lesion shape due to boiling (20 and 30 s), and shrinkage of the lesion soon after HIFU exposure (40 s). Two gel samples were sonicated from the right at ambient static pressure for 30 s with equal acoustic power of 42 W and different illumination either from the left-hand side toward the transducer (frames on the left) or with scattered backlight (frames on the right). Small bubbles of the order of 300 μm were present and visible as dark shadows in the lesion under backlighting conditions at 15 s, but large boiling bubbles of the order of 3 mm were obvious after 20 s.

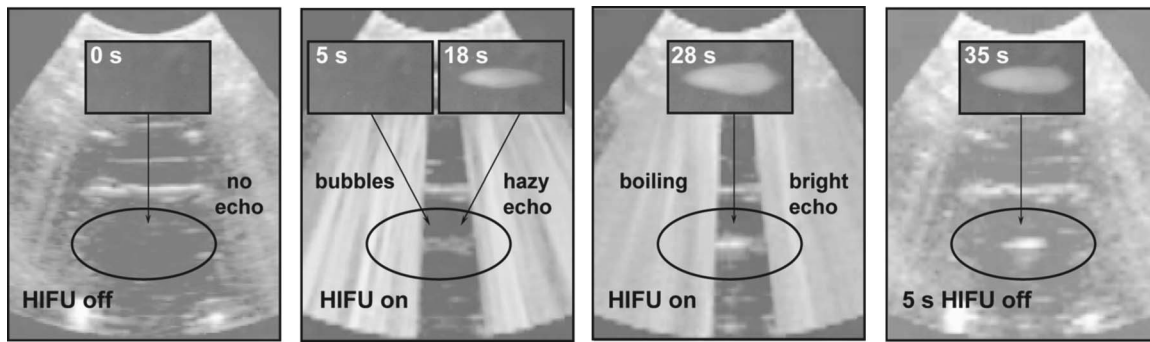


FIG. 9. Simultaneous visualization of the effect of HIFU on nondegassed gel with B-mode imaging and CCD video capture (inset) during 30 s exposure, no overpressure, 36.5 W average acoustic power, and 72% duty cycle. The HIFU transducer was on the right-hand side, lighting was from the left-hand side, and the diagnostic probe was on the back side of the chamber (on the top in the images). The HIFU focal region in the gel is initially hypoechogenic. During HIFU, interference covers all but the center of the image. At the focus, first a weakly brightened zone is seen, and then a strongly echogenic region appears as bubbles become visible in the lesion and the lesion begins to distort dramatically.

samples treated for 30 s with equal acoustic power of 42 W and different illumination, either through the left acrylic window of the chamber towards the HIFU transducer (frames on the left), or with diffuse backlight on the distal window (frames on the right). The power level of the transducer was chosen experimentally to provide clear observations of all stages of lesion development, i.e., lesion inception, symmetric growth, and start of boiling, within the chosen exposure time of 30 s. Side light provided better visualization of the lesion shape and size, and the internal structure of the lesion was better seen when backlit. An LED lamp can be seen (as a blurred zone since the LED was not inside the chamber and outside the camera's depth of field) in the top right corner of each frame indicating when HIFU exposure was in progress. Exposure times are given on the left-hand set of frames and characteristic stages of lesion development in gel are commented on the right-hand set of the frames. The lesion became visible after 9 s of HIFU, it grew symmetrically (15 s) as a thin cigar shape until a large boiling bubble of about 2–3 mm size burst from the middle of the lesion (20 s). The bubble was clearly seen when backlit and was detected as a bright flash when lit from the side (the sidelit and backlit images are taken from different exposure sequences). Boiling bubbles continued to form and break inside the lesion, which started to distort and grow toward the transducer. The heat diffused outward creating the appearance of an evenly denatured lesion in an image obtained with the side light. A typical drop-shaped lesion was formed by the end of the exposure (30 s) with an inhomogeneous bubbly internal structure in the middle (only visible with backlight) and a smoother structure closer to the edges. After HIFU was turned off, the cavities that had formed due to boiling inside the lesion contracted, and the lesion shrank (40 s). The results of this experiment clearly showed the process of boiling in the gel and production of an inhomogeneous internal structure of lesion, very similar to (vaporized) cavities typically observed in overheated tissues (Fig. 4). These results give additional evidence that boiling is responsible for distortion of the lesion shape, and results in rapid growth from the focus towards the transducer. It is important to note that *the experiment was performed in the presence of cavitation but no distortion of the lesion was observed before boiling started*. Cavitation

was not experimentally detected in this set of experiments because microbubbles cannot be visualized directly, but the acoustic power applied was about three times higher than the cavitation threshold power obtained using PCD measurements in an equivalent setup outside the hyperbaric chamber.

In order to detect microbubble cavitation using a clinically convenient method and compare its appearance with boiling signatures, in the next experiments the results of direct visualization of lesion formation were correlated with diagnostic ultrasound imaging. Microbubbles are strong scatterers of ultrasound, and their presence during HIFU exposure can potentially be seen on B-mode diagnostic ultrasound images, though the absence of B-mode detection cannot guarantee the absence of cavitation.³⁴ Shown in Fig. 9 is a sequence of B-mode images obtained concurrently with video frames during a 30 s exposure at atmospheric pressure, with 36.5 W average acoustic power, and 72% duty cycle. The gel was heated by HIFU from the right-hand side, lighting was from the left-hand side, and the diagnostic probe was mounted on the back side of the chamber (Fig. 2) oriented with the image plane parallel to the HIFU beam axis so as to view the focal region longitudinally. A weakly echogenic region appeared on the B-mode image immediately after HIFU was turned on and remained in the image through the stages of “no lesion” (5 s) and “cigar-shape thermal lesion” (18 s) observed in the gel. A bright echogenic region was coincident with the start of boiling (start of drop-shaped lesion distortion, 28 s) and persisted after HIFU was off and the lesion shrank (35 s).

These results indicate that cavitation microbubbles may be seen on the B-mode image as a slight increase in echogenicity, even prior to lesion inception. However, this weak echogenicity (enhancement) was not seen in all gel samples exposed under similar conditions. The weak brightening was only perceptible for gels with the most nearly homogeneous and initially scatterer-free structure in the focal area (frame at 0 s), and the possibility remains that in some cases cavitation bubbles were not sufficiently numerous to be detected by a typical observer using a medical B-mode ultrasound scanner. The inhomogeneous structure of tissue would make direct B-mode visualization of the focal region of HIFU preceding boiling even more challenging;³⁴ nevertheless, more

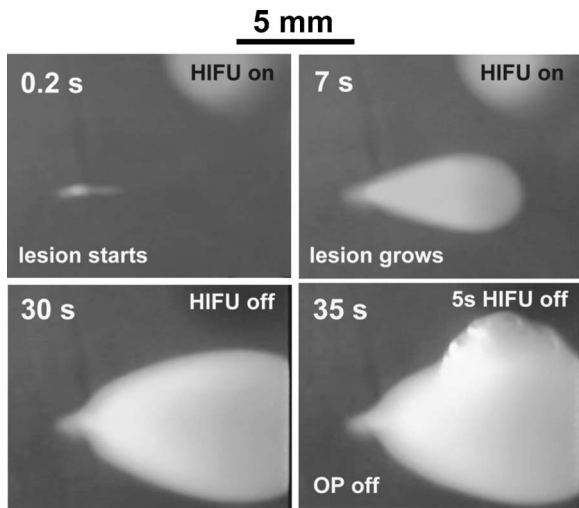


FIG. 10. Development of superheated lesion in degassed gel during 30 s exposure to HIFU under slightly elevated static pressure of 20 bars, and boiling explosion of bubbles from the lesion caused by overpressure (OP) release 5 seconds after HIFU was turned off. The HIFU transducer was on the right-hand side. Acoustic power of the source was 77 W with 100% duty cycle. An LED in the upper right-hand corner of the frames indicates when HIFU was being applied. The explosion of bubbles is seen as the superheated lesion suddenly boils out.

sophisticated methods of processing backscattered ultrasound have detected cavitation at the very early stage of HIFU treatment, before boiling.^{8,9}

Following boiling, the strongly hyperechogenic region persisted in B-mode observations for more than 1 minute after the treatment, which was consistent with previous numerical and experimental results for tissue.^{19,25} The mechanism for dissipation of the echogenicity has been hypothesized to be cooling and shrinkage of the vapor cavities created by boiling, filling of remaining matrix voids with liquid, and dissolution of residual gas. The gel is stiffer and less viscoelastic than tissue and may preserve the shape of cavities formed by bubble growth longer than tissue.

Further experiments were conducted under elevated static pressure. To test the hypothesis that large visible bubbles and ensuing lesion distortion in the gel were due to boiling, and not to HIFU-induced cavitation, one gel sample was treated for 30 s under slightly elevated static pressure of 20 bars and a very high acoustic power of 77 W with 100% duty cycle, exposure conditions which were numerically predicted to lead to boiling temperatures. Because boiling temperature increases with static pressure, a pressurized liquid brought to the boiling point would be superheated with respect to normal atmospheric conditions. Overpressure release after sonication was utilized to confirm boiling inside the lesion. Figure 10 illustrates fast inception of the lesion in gel (0.2 s), lesion growth from the focal spot toward the transducer in a typical tadpole shape caused by boiling (7 s), final lesion shape when HIFU was turned off (30 s), and an explosion of bubbles from the lesion volume when the chamber was depressurized 5 seconds after the end of HIFU exposure (35 s). An LED light in the upper right corner of the frames indicates when the HIFU power was being delivered. Eruptive boiling immediately following decrease in pressure con-

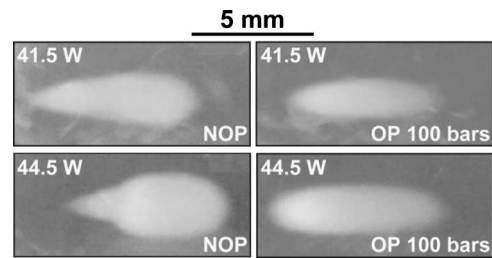


FIG. 11. Comparison of final lesions obtained in degassed gel after 30 s exposure to HIFU (cw regime) under atmospheric static pressure (frames on the left) and under overpressure of 100 bars (frames on the right) with 41.5 and 44.5 W acoustic power chosen below and above the shock formation transition level, respectively. The HIFU transducer was on the right-hand side. Under overpressure the lesions grew symmetrically around the focus to the similar size but different shape than the ones formed without overpressure which were distorted by the effects of boiling bubbles.

firmed that the lesioned zone had indeed been raised to the boiling point (at 20 bars over atmospheric pressure).

To examine the effect of overpressure on lesion development and on the onset and characteristics of strong B-mode brightening near the HIFU focal region, gradually increased overpressure levels of 5, 10, 20, and 100 bars were applied in the next series of experiments. Acoustic power from 41.5 to 47 W and 100% duty cycle was used for direct visualization; these levels were chosen because field models indicate that the pressure waveform in the focal region exhibits a rapid transition in this power interval from somewhat distorted (due to nonlinearity) to strongly shocked. In a second sequence of static pressure experiments, 32 W average acoustic power with 50% duty cycle (64 W power during on-time) was used with interleaved B-mode imaging. No weak echoes related to microbubbles were seen on the B-mode images preceding lesion inception and during symmetric lesion growth in any of these overpressure experiments, likely indicating that cavitation was reduced to undetectable levels. Visual detection of boiling bubbles coincided with the appearance of very bright echoes in the focal region in B-mode images, further supporting the hypothesis that only boiling produces such brightening. Higher levels of HIFU, or longer exposures at a given power level, were required to reach boiling for each successive increase in static pressure, consistent with the fact that the boiling point increases with ambient pressure.³⁵ Moderate overpressure of 5 and 20 bars did not prevent drop-shaped distortion of the lesion shape due to boiling, just as was observed at atmospheric pressure, but it was noted that no lesion distortion occurred with the relatively high overpressure of 100 bars, though boiling was clearly evident. This result is illustrated in Fig. 11, and discussed below.

Final lesions obtained after 30 s of exposure with and without overpressure of 100 bars are presented for comparison in Fig. 11. Lesion inception times (time of first visible discoloration of the gel) were 6 s without overpressure and 14 s with overpressure, at 41.5 W acoustic power; 4 s without overpressure and 10 s with overpressure for 44.5 W. As expected, lesions appeared earlier using higher HIFU power (for a given ambient pressure), and earlier for lower ambient pressure (at a given HIFU power) due to microbubble cavitation which is completely suppressed with 100 bars over-

pressure. Without overpressure, boiling began after lesion inception (at 18 s for 41.5 W, and at 7 s for 44.5 W) and the lesions grew asymmetrically toward the transducer. The lesions appeared substantially later under overpressure and grew symmetrically around the focus without distortion. Perhaps surprisingly, boiling was observed in the 44.5 W/100 bar experiment, but the bubbles were not persistent (they collapsed rapidly) nor was there any tadpole distortion of the lesion shape, as observed in the other cases of lower overpressure in which boiling occurred. The likely explanation is that because the pressure was at 100 bars, the boiling point (reached at the focus) was near 300 °C,³⁵ and consequently the temperature gradient between the beam axis and the edge of the lesion (near 60 °C) was very high. Bubbles expanding from the axis would cool rapidly, and collapse back into a condensed phase before they persisted long enough to distort the local heating pattern significantly. Similar bubble behavior can be observed on the hot walls of a pan of water that is being heated on a stove, before the average water temperature approaches 100 °C, the walls are much hotter than the boiling point, and effectively superheat water at the boundary and expand explosively only to collapse upon rapid cooling. It is also interesting to note, that in the boiling regime (with 44.5 W) the final lesions obtained after the 30 s exposure with and without overpressure were very different in shape, but the lesion volumes were almost the same (Fig. 11, bottom row). With no overpressure the boiling bubbles make the lesion grow very rapidly at first, scattering the acoustic field and distorting and growing the lesion toward the transducer, and then slowing overall lesion growth rate due to shielding of the focal region where maximum heat deposition would occur.

Final experiments with overpressure were conducted with the goal of isolating the effect of acoustic nonlinearity

from the effect of microbubbles in enhancing heat deposition in the gel. The level of overpressure was set to exceed the maximum negative pressure of HIFU which was obtained from the acoustic waveforms simulated numerically for given experimental conditions (Fig. 12). Two different HIFU protocols were applied, one with lower amplitude continuous waves (32 W acoustic power and 100% duty cycle, here called “low amplitude” heating, referring in relative terms to the degree of nonlinearity in the acoustic propagation regime), and another using higher amplitude pulses (64 W pulse acoustic power and 50% duty cycle; “high amplitude” heating regime). A time-average acoustic power of 32 W was maintained for both protocols, expected to produce the same heating results for all cases if nonlinear phenomena were not involved. Images of final lesions formed in gel after 30 s exposures to HIFU under atmospheric pressure and 100 bars overpressure, as well as the focal waveforms modeled for the corresponding two power levels, are presented in Fig. 12. Several observations from this experiment provide insight to the effects of cavitation, acoustic nonlinearity, and the effect of heating to the point of boiling.

In the case of “low amplitude” heating and no overpressure (NOP) the lesion started forming in 15 seconds and grew symmetrically without distortion up to the end of exposure (left-hand frame in the top row of Fig. 12). No visible bubbles were detected. As expected from the use of higher peak pressures, for “high amplitude” heating and no overpressure (NOP) the lesion started much earlier (in 3 seconds), and also grew symmetrically until bubbles appeared in the video image (8 s of exposure) at which time the lesion began to distort in shape and migrate toward the transducer (right-hand frame in the top row).

With overpressure (OP) of 100 bars and “low amplitude” heating the lesion started later than without overpres-

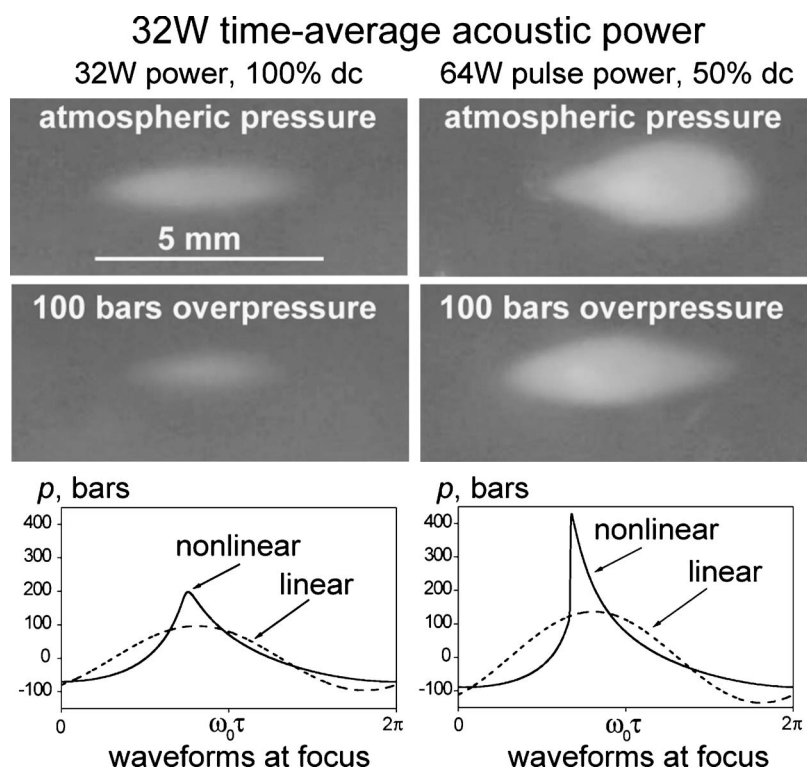


FIG. 12. Final lesions formed in degassed gel under standard atmospheric static pressure (1 bar) and under overpressure (100 bars) after 30 s exposure to HIFU of lower (with 100% duty cycle) and higher (with 50% duty cycle) peak pressure and equal average acoustic power of 32 W. The HIFU transducer was on the right-hand side. Corresponding waveforms are modeled at focus with and without accounting for the effects of nonlinear propagation. The largest change in lesion size is observed by comparing the cases with a change in acoustic pressure, rather than the cases for which only the static pressure was changed. The first comparison isolates the role of acoustic nonlinearity (for high static pressure), whereas the latter comparison isolates the role of cavitation; these observations indicate that nonlinear propagation played a larger role in increasing HIFU heating than did cavitation.

sure (24 seconds of exposure) and had smaller final size (left-hand frame in the bottom row), indicating that, even at reduced acoustic pressure amplitudes, cavitation was clearly contributing to heating (at ambient static pressure). “High amplitude” heating under overpressure resulted in lesion inception in 8 seconds, which was substantially later than without overpressure (again indicating the role of cavitation), but occurred much earlier than in the “low amplitude” OP regime (indicating the importance of acoustic nonlinearity). Again, as shown in Fig. 11 (bottom row), the final size of the “high” OP lesion (right-hand frame in the bottom row) was almost the same as for the “high” NOP lesion, but the shape was different. Although it started later due to the complete suppression of cavitation, the OP lesion grew more rapidly and retained a symmetric shape even after boiling due to strong temperature gradient near the acoustic axis that rapidly cooled expanding vapor bubbles and due to the suppression of boiling bubble growth by overpressure.

The fact that lesion inception times with overpressure were longer than without overpressure for both “low” and “high” heating regimes indicates that cavitation microbubbles not apparent to the eye, but detected in B-mode images (Fig. 9), and measured by PCD, contributed to the enhancement of gel heating. This evidence is consistent with the previously reported results that once the nuclei gas bubbles are activated by HIFU and cavitate, enhanced heating is observed.^{14,16,22} Suppression of cavitation by static overpressure has been used previously.^{36,37} For the conditions in gel experiments described here, the lesion inception time and final lesion size changed most between the “low” (weakly nonlinear) and the “high” (strongly nonlinear) acoustic intensity regimes, for both ambient and overpressure conditions, one of which completely suppressed cavitation activity. Therefore, we deduce that the effect of acoustic nonlinearity was a major contributor to enhanced heating and accelerated lesion formation, though cavitation also played a role at standard atmospheric pressure.

Many points can be summarized from the overpressure experiments. Overpressure raises the boiling temperature and significantly delayed the appearance of large bubbles—observed simultaneously visually and as a strong rise in echogenicity on B-mode ultrasound—which is consistent with the evidence of the preceding sections that these bubbles (and bright-up) are due to boiling. Explosive large bubble formation upon the release of overpressure was interpreted as boiling resulting from a superheated condition following pressure decrease, and was further evidence that the large, highly echogenic bubbles are the result of boiling, not cavitation. Lesions began to distort visibly only after boiling was evident, and since bubbles continued to appear in the lesion as it migrated and distorted, this result supports previous evidence that reflection from these large bubbles causes the lesion distortion. It is interesting to note that until boiling started, no distortion occurred; yet, cavitation was clearly present in the absence of overpressure, because lesion inception times lengthened substantially with overpressure, for constant HIFU parameters. Thus we conclude that microbubble cavitation, though present, did not result in observable lesion distortion in any of the experiments described

here. A subtle, weakly enhanced echogenic region appeared on B-mode images in and near the HIFU focal region at atmospheric pressure prior to boiling, but did not appear when the experiment was repeated with overpressure. From this result we infer that the subtle enhancement in B-mode was evidence of microbubbles; the weak enhancement often appears to blur the original speckle pattern, and gives the impression of a foggy or hazy overlay on the image rather than an increase in brightness. We (and others) have previously seen evidence of microbubbles before detection of a pronounced hyperechogenic region on B-mode. Cavitating microbubbles have yielded accelerated heating in HIFU experiments with these gels and other gel phantoms.¹⁶ In support of enhanced heating due to cavitation we observed that lesions created under overpressure took longer to form than at 1 bar. This result we interpret as evidence that suppression of microbubbles by overpressure reduced heating by cavitation and/or removed the excess acoustic absorption caused by the presence of the bubbles in the gel. In general, the overpressure experiments indicated that, for the range of HIFU intensities that encompassed and exceeded the transition from weakly nonlinear to strongly shocked waveforms, the effect of acoustic nonlinearity was larger than that of microbubble cavitation on the acceleration of lesion formation. Specifically, strongly nonlinear propagation with overpressure (completely suppressing cavitation) ultimately produced the largest lesion, and the lesion remained symmetric and centered at the focus because the shielding effect of boiling bubbles was also suppressed. The HIFU intensities used in ablative therapy are high and acoustic fields are likely to be in the range of strongly nonlinear propagation.

V. CONCLUSIONS

The effects of acoustic nonlinearity, cavitation, and boiling on the dynamics of lesion formation in protein-containing gel phantom exposed to HIFU were investigated experimentally and theoretically in different regimes. Both cavitation and acoustic nonlinearity have been previously proven to enhance heating. One of the goals of this research was to examine the respective roles of these phenomena separately, and especially to use static overpressure to evaluate the role of nonlinear propagation alone in heating of the gel phantom, and to separate the effects of boiling from those of microbubble cavitation.

Our experimental observations confirmed expectations developed using nonlinear acoustic simulations, in particular, the use of high-amplitude tone bursts instead of cw waves of equal acoustic energy leads to accelerated lesion formation and results in larger lesions. Nevertheless, at an ambient pressure that is less than the peak negative pressure of HIFU, cavitation microbubbles also contribute to enhanced heating in gel. This was confirmed here by comparing rates of lesion formation with and without static overpressure that exceeded negative peak pressure and hence completely suppressed cavitation; the cavitation threshold for the gel has been exceeded at standard atmospheric pressure even for weakly nonlinear waveforms. For acoustic power levels near the relatively sharp transition for development of acoustic

shocks near the focus, acoustic nonlinearity was found to be the dominant mechanism for accelerating heating, that is, until boiling occurs. The evidence for this conclusion was that the metrics used for monitoring the acceleration of lesion formation, lesion inception times (shorter for high amplitude pulses), and lesion volumes (larger for high amplitude pulses), were essentially independent of gel gas content or static pressure. The effect of nonlinear acoustic enhancement of lesion production is most pronounced in a narrow zone around the focal axis where shocks form, and thus rapid transverse displacement of the ultrasound transducer (scanning to form lesion stripes) was an excellent approach to visualizing the effect of this enhancement. While static lesion formation is slowed as soon as boiling bubbles appear, scanning permits moving the heat source away from the boiling region before the vapor bubbles have much time to grow and disrupt the highly focused field.

It was shown that several previously observed phenomena were due to boiling in the gel, and not to cavitation, these include greatly increased echogenicity (“bright-up”) observed with B-mode ultrasound that is often used to monitor HIFU treatment, distortion of lesions into drop or “tadpole” shape, and rapid lesion growth toward the transducer with associated shielding of the focal zone. Evidence for boiling included the results of nonlinear models of acoustic propagation and heating for the gel experiments, which produced temperatures greater than the boiling point only for those experimental conditions when large bubbles were observed. Furthermore, the sudden creation of persistent and large bubbles (2–3 mm), the similar increase in bubble appearance time with overpressure (that raises the boiling point), and the explosive creation of such bubbles with depressurization of HIFU-heated gel, provide additional support that boiling was responsible. Lesion formation for the gel was essentially instantaneous above 60 °C and always preceded the appearance of visible bubbles.

Highly efficient heating leading to boiling bubble formation was observed above a sharply determined intensity threshold that coincided with the numerically estimated threshold for shock formation in the focal region. This numerical estimate was made without including any factors arising from potential cavitation activity, such as increased values of absorption, for example. Visually observable bubbles first formed in a narrow zone along the HIFU axis (visualized by the lesion) which is consistent with superfocusing by nonlinear wave propagation.¹³ The formation of large bubbles which are strong reflectors of ultrasound also coincided with the appearance of a brightly echogenic region on B-mode ultrasound images, and triggered visible change of the shape of ensuing lesion growth and migration toward the transducer. No lesion distortion was observed when boiling bubbles were prevented from growing to a large size by overpressure or before boiling bubbles were observed, even for conditions when microbubble cavitation was occurring. The presence of large bubbles enhances lesion growth due to strong reflections, but it also screens the focal zone of HIFU. With high amplitude-shocked waves and with overpressure used to raise the boiling point and prevent the shielding effect of boiling bubbles, the lesions grew rapidly but sym-

metrically around the focus to a large size on the same order as that developed with distortion under standard static pressure.

A subtle increase in echo brightness, associated with blurring or a “hazy” appearance, was observed on B-mode images preceding lesion inception and leading up to boiling. This weakly echogenic region was interpreted as evidence of cavitation microbubbles because it was not observed with overpressure, given the same HIFU exposure conditions. With overpressure, lesion inception time was always delayed with respect to the experiments conducted at standard pressure. These observations were interpreted as evidence for cavitation, and cavitation-induced heating, and that the hazy spot is a signature of active cavitation detection using B-mode ultrasound. Since the haze preceded visible lesion formation, more sensitive backscatter processing algorithms to detect and quantify these microbubbles may be useful for targeting and monitoring HIFU treatment.

The experimental results thus show that both cavitation (microbubble dynamics) and nonlinear ultrasound propagation accelerate lesion inception and growth in the gel phantom. By suppressing cavitation with overpressure, and by trading pulse amplitude against duration to accentuate acoustic nonlinearity, nonlinear propagation was observed to be the larger effect. The importance of acoustic nonlinearity in the gel phantom is due to the relatively small value of the attenuation coefficient. Linear attenuation in biological tissue is about 3 times higher than in gel, thus nonlinear gain in heat deposition due to formation of shocks will be lower. However, the results of modeling in tissues at typical HIFU intensities also predict formation of shocks and associated temperature rise above 100 °C, suggesting that nonlinear propagation effects will also be very important for HIFU exposures in biological media.^{13,21} The occurrence of boiling in tissue is supported by many experimental observations of vaporized cavities in tadpole-shaped lesions in real tissues.

Nonlinear propagation effects produced in higher peak acoustic pressure regimes, balanced with lower duty cycle to maintain the same time-average transducer power, would improve the efficiency of HIFU treatment by permitting faster transducer scan rates and consequently shorter treatment times. Additional benefits include smaller energy requirements for portable devices and convenient time windows for ultrasonic imaging of treatment when HIFU is off.

ACKNOWLEDGMENTS

The work at the Center for Industrial and Medical Ultrasound (CIMU) at the Applied Physics Laboratory of the University of Washington has been supported by grants from the National Space Biomedical Research Institute (SMS00203) in consortium agreement with the National Aeronautics and Space Administration, the National Science Foundation Grant No. (BES-0002932), and the National Institutes of Health Grant No. (CA83244). The work in the Department of Acoustics at Moscow State University has been supported by the CRDF, RFBR, ONRIFO, and NIH Fogarty. The authors gratefully acknowledge the assistance

of Michael Canney for arranging and performing PCD measurements of cavitation activity in gels.

- ¹*Proceedings of the 3rd International Symposium on Therapeutic Ultrasound* (June 22–25, 2003, Lyon, France), edited by J.-Y. Chapelon and C. Lafon.
- ²N. T. Sanghvi and R. H. Hawes, “High-intensity focused ultrasound,” *Gastrointest Endosc Clin. N. Am.* **4**, 383–395 (1994).
- ³S. Vaezy, X. Shi, R. W. Martin, E. Chi, P. I. Nelson, M. R. Bailey, and L. A. Crum, “Real-time visualization of focused ultrasound therapy,” *Ultrasound Med. Biol.* **27**, 33–42 (2000).
- ⁴M. R. Bailey, V. A. Khokhlova, O. A. Sapozhnikov, S. G. Kargl, and L. A. Crum, “Physical mechanisms of the therapeutic effect of ultrasound,” *Acoust. Phys.* **49**, 437–464 (2003).
- ⁵F. Wu, W.-Z. Chen, J. Bai, J.-Z. Zou, Z.-L. Wang, H. Zhu, and Z.-B. Wang, “Pathological changes in human malignant carcinoma treated with high-intensity focused ultrasound,” *Ultrasound Med. Biol.* **27**, 1099–1106 (2001).
- ⁶F. Wu, Z.-B. Wang, W.-Z. Chen, J.-Z. Zou, J. Bai, H. Zhu, K.-Q. Li, F.-L. Xie, C.-B. Jin, H.-B. Su, and G.-W. Gao, “High intensity focused ultrasound for extracorporeal treatment of solid carcinomas: four-year Chinese clinical experience,” in *Proceedings of the 2nd International Symposium on therapeutic ultrasound* (July 29–August 1, 2002, Seattle, USA), edited by M. A. Andrew, L. A. Crum, and S. Vaezy, pp. 34–43.
- ⁷S. Vaezy, M. Andrew, P. Kaczkowski, and L. Crum, “Image-guided acoustic therapy,” *Annu. Rev. Biomed. Eng.* **3**, 375–390 (2001).
- ⁸P. Phukpattaranont and E. S. Ebbini, “Post-beamforming second-order Volterra filter for pulse-echo ultrasonic imaging,” *IEEE Trans. Ultrason. Ferroelectr. Freq. Control* **50**, 987–1001 (2003).
- ⁹A. Anand and P. J. Kaczkowski, “Monitoring formation of high intensity focused ultrasound (HIFU) induced lesions using backscattered ultrasound,” *ARLO* **5**, 88–94 (2004).
- ¹⁰R. Souchon, L. Soualmi, M. Bertrand, J.-Y. Chapelon, F. Kallel, and J. Ophir, “Ultrasonic elastography using sector scan imaging and radial compression,” *Ultrasonics* **40**, 867–871 (2001).
- ¹¹K. Hynynen, W. R. Freund, H. E. Cline, A. H. Chung, R. D. Watkins, J. P. Vetro, and F. A. Jolesz, “A clinical, noninvasive, MR imaging-monitored ultrasound surgery method,” *Radiographics* **16**, 185–195 (1996).
- ¹²K. Hynynen, “Demonstration of enhanced temperature elevation due to nonlinear propagation of focused ultrasound in dog’s thigh muscle *in vivo*,” *Ultrasound Med. Biol.* **13**, 85–91 (1987).
- ¹³E. A. Filonenko, G. ter Haar, I. Rivens, and V. A. Khokhlova, “Prediction of ablation volume for different HIFU exposure regimes,” in *Proceedings of the 3rd International Symposium on Therapeutic Ultrasound* (June 22–25, 2003, Lyon, France), edited by J.-Y. Chapelon and C. Lafon, pp. 268–274.
- ¹⁴K. Hynynen, “The threshold for thermally significant cavitation in dog’s thigh muscle *in vivo*,” *Ultrasound Med. Biol.* **17**, 157–169 (1991).
- ¹⁵L. A. Crum and G. M. Hansen, “Growth of air bubbles in tissue by rectified diffusion,” *Phys. Med. Biol.* **27**, 413–417 (1982).
- ¹⁶R. G. Holt and R. A. Roy, “Measurements of bubble-enhanced heating from focused, MHz-frequency ultrasound in a tissue-mimicking material,” *Ultrasound Med. Biol.* **27**, 1399–1412 (2001).
- ¹⁷P. Meaney, M. D. Cahill, and G. ter Haar, “The intensity dependence of lesion position shift during focused ultrasound surgery,” *Ultrasound Med. Biol.* **26**, 441–450 (2000).
- ¹⁸F. Chavrier, J. Y. Chapelon, A. Gelet, and D. Cathignol, “Modeling of high-intensity focused ultrasound-induced lesions in the presence of cavitation bubbles,” *J. Acoust. Soc. Am.* **108**, 432–440 (2000).
- ¹⁹M. R. Bailey, L. N. Couret, O. A. Sapozhnikov, V. A. Khokhlova, G. ter Haar, S. Vaezy, X. Shi, R. Martin, and L. A. Crum, “Use of overpressure to assess the role of bubbles in focused ultrasound lesion shape,” *Ultrasound Med. Biol.* **27**, 696–708 (2000).
- ²⁰T. G. Muir and E. L. Carstensen, “Prediction of nonlinear acoustic effects at biomedical frequencies and intensities,” *Ultrasound Med. Biol.* **6**, 345–357 (1980).
- ²¹E. A. Filonenko and V. A. Khokhlova, “Effect of acoustic nonlinearity on heating of biological tissue induced by high intensity focused ultrasound,” *Acoust. Phys.* **47**, 541–549 (2001).
- ²²Y. Kaneko, T. Higaki, T. Maruyama, and Y. Matsumoto, “The effect of microbubbles as a heat transducer,” in *Proceedings of the 3rd International Symposium on Therapeutic Ultrasound* (June 22–25, 2003, Lyon, France), edited by J.-Y. Chapelon and C. Lafon, pp. 55–60.
- ²³L. A. Crum and W. Law, “The relative roles of thermal and nonthermal effects in the use of high intensity focused ultrasound for the treatment of benign prostatic hyperplasia,” *Proceedings of the 15th International Congress on Acoustics* (Trondheim, Norway, 1995), pp. 315–318.
- ²⁴N. A. Watkin, G. R. ter Haar, and I. Rivens, “The intensity dependence of the site of maximal energy deposition in focused ultrasound surgery,” *Ultrasound Med. Biol.* **22**, 483–491 (1996).
- ²⁵F. J. Fry, N. T. Sanghvi, R. S. Foster, R. Bihrlé, and C. Hennige, “Ultrasound and microbubbles: their generation, detection, and potential utilization in tissue and organ therapy—experimental,” *Ultrasound Med. Biol.* **21**, 1227–1237 (1995).
- ²⁶F. L. Lizzi, D. J. Coleman, J. Driller, R. H. Silverman, B. Lucas, and A. Rosado, “A therapeutic ultrasound system incorporating real-time ultrasonic scanning,” *Ultrasonics Symposium* (Institute of Electrical and Electronic Engineers, New York, 1986), pp. 981–984.
- ²⁷C. Lafon, P. Kaczkowski, S. Vaezy, M. Noble, and O. Sapozhnikov, “Development and characterization of an innovative synthetic tissue-mimicking material for high intensity focused ultrasound (HIFU) exposures,” *Proceedings of IEEE Ultrasonics Symposium*, 2001, pp. 1295–1298.
- ²⁸O. A. Sapozhnikov, V. A. Khokhlova, T. V. Sinilo, E. A. Filonenko, and L. A. Crum, “Thermal effects of sawtooth waveform HIFU in tissue phantoms,” *Proceedings of the 17th International Congress on Acoustics* (Rome, Italy, Sept. 2–7, 2001).
- ²⁹M. O’Donnell, E. T. Janes, and J. G. Miller, “Kramers-Kronig relationship between ultrasonic attenuation and phase velocity,” *J. Acoust. Soc. Am.* **69**, 696–701 (1981).
- ³⁰V. A. Khokhlova, R. Souchon, J. Tavakkoli, O. A. Sapozhnikov, and D. Cathignol, “Numerical modeling of finite amplitude sound beams: Shock formation in the nearfield of a cw plane piston source,” *J. Acoust. Soc. Am.* **110**, 95–108 (2001).
- ³¹S. Sapareto and W. Dewey, “Thermal dose determination in cancer therapy,” *Int. J. Radiat. Oncol., Biol., Phys.* **10**, 787–800 (1984).
- ³²G. ter Haar, “Ultrasound focal beam surgery,” *Ultrasound Med. Biol.* **21**, 1089–1100 (1995).
- ³³N. T. Sanghvi, F. J. Fry, R. Bihrlé, R. S. Foster, M. H. Phillips, J. Syrus, A. Zaitsev, and C. Hennige, “Microbubbles during tissue treatment using high intensity focused ultrasound,” *Proceedings of IEEE 95 UFFC Symposium*, 1995, pp. 1249–1253.
- ³⁴B. A. Rabkin, V. Zderic, and S. Vaezy, “Hyperecho in ultrasound images of HIFU therapy: involvement of cavitation,” *Ultrasound Med. Biol.* **31**, 947–956 (2005).
- ³⁵*Handbook of Chemistry and Physics*, edited by R. C. Weast (CRC Press, Boca Raton, FL, 1985), pp. D186–D187.
- ³⁶W. J. Fry, D. Tucker, F. J. Fry, and V. J. Wulff, “Physical factors involved in ultrasonically induced changes in living systems: II. Amplitude duration relation and the effect of hydrostatic pressure for nerve tissue,” *J. Acoust. Soc. Am.* **23**, 364–368 (1951).
- ³⁷P. P. Lele, “Effects of ultrasound on ‘solid’ mammalian tissues and tumors *in vivo*,” *Ultrasound: Medical Applications, Biological Effects and Hazard Potential* (Plenum, New York, 1986), pp. 275–306.